Experimental Brain Research (2019) 237:257–271
https://doi.org/10.1007/s00221-018-5422-0

RESEARCH ARTICLE

Local dynamic stability in temporal pattern of intersegmental coordination during various stride time and stride length combinations

Benio Kibushi[1,2] · Toshio Moritani[3] · Motoki Kouzaki[1]

Received: 6 July 2018 / Accepted: 29 October 2018 / Published online: 2 November 2018

Abstract
For the regulation of walking speed, the central nervous system must select appropriate combinations of stride time and stride length (stride time–length combinations) and coordinate many joints or segments in the whole body. However, humans achieve both appropriate selection of stride time–length combinations and effortless coordination of joints or segments. Although this selection of stride time–length combination has been explained by minimized energy cost, it may also be explained by the stability of kinematic coordination. Therefore, we investigated the stability of kinematic coordination during walking across various stride time–length combinations. Whole body kinematic coordination was quantified as the kinematic synergies that represents the groups of simultaneously move segments (intersegmental coordination) and their activation patterns (temporal coordination). In addition, the maximum Lyapunov exponents were utilized to evaluate local dynamic stability. We calculated the maximum Lyapunov exponents in temporal coordination of kinematic synergies across various stride time–length combinations. The results showed that the maximum Lyapunov exponents of temporal coordination depended on stride time–length combinations. Moreover, the maximum Lyapunov exponents were high at fast walking speeds and very short stride length conditions. This result implies that fast walking speeds and very short stride length were associated with lower local dynamic stability of temporal coordination. We concluded that fast walking is associated with lower local dynamic stability of temporal coordination of kinematic synergies.

Keywords Maximum Lyapunov exponents · Motor control · Kinematic synergies · Singular value decomposition · Stride time · Stride length

Introduction

Although humans can achieve a given walking speed by various combinations of stride time and stride length (stride time–length combination), we ordinarily select similar stride time–length combinations to modulate walking speed. Specifically, we typically select a preferred stride time–length combination at a given walking speed, whereas exceedingly long stride length/times or very short stride length/times are not selected for the modulation of walking speeds. An explanation for this preferred stride time–length combination is that selection of an optimal stride time–length combination or step width minimizes energy cost (Bertram and Ruina 2001; Donelan et al. 2001; Kuo 2001). However, the manner in which stride time–length combination affects joint or limb segment mechanics is not considered in this regard, because the energy cost is associated with whole body mechanics. Investigating how stride time–length combinations affect joint or limb segment mechanics is needed for identification of control of stride time or stride length.

The coordination patterns of limb segments during walking have been previously investigated to examine joint or segment mechanics. In a three-dimensional space that was constructed by the time course of the rotation angle of limb

✉ Motoki Kouzaki
kouzaki.motoki.4x@kyoto-u.ac.jp

[1] Laboratory of Neurophysiology, Graduate School of Human and Environmental Studies, Kyoto University, Yoshida-nihonamatsu, Sakyo-ku, Kyoto, Kyoto 606-8501, Japan

[2] Research Fellow of the Japan Society for the Promotion of Science, Kojimachi Business Center Building, 5-3-1 Kojimachi, Chiyoda-ku, Tokyo, Japan

[3] School of Health and Sport Sciences, Chukyo University, 101-2 Yagoto Honmachi, Showa-ku, Nagoya, Aichi, Japan

segments, the three-dimensional trajectory of the elevation angle lies close to a plane (Borghese et al. 1996; Lacquaniti et al. 1999; Courtine and Schieppati 2004), and this planar law may reflect intersegmental coordination. The planar law of intersegmental coordination has been observed at different walking speeds (Bianchi et al. 1998), forward or backward directions (Grasso et al. 1998), and different levels of body weight unloading (Ivanenko et al. 2002). Thus, intersegmental coordination has been broadly observed in various types of locomotion. In analysis of the planar law, the characteristics of intersegmental coordination are quantified by spatial characteristics of the plane (e.g., planarity or orientation of the plane). Therefore, it is difficult to investigate temporal characteristics in the planar law of intersegmental coordination. Analysis of kinematic synergies might solve this problem. Groups of simultaneously move segments (intersegmental coordination) and their activation patterns (temporal coordination) have been investigated as kinematic synergies using the matrix factorization technique (Funato et al. 2010, 2015; Sano and Wada 2017; Ivanenko et al. 2007). Seven elevation angles of segments during walking could be characterized by a few kinematic synergies (Funato et al. 2010, 2015). Previous studies have shown that extracted kinematic synergies are related to a change in limb axis orientation or a change in limb axis length (Funato et al. 2010, 2015). Thus, analysis of kinematic synergies enables identification of segment mechanics as coordination patterns.

The significance of the temporal pattern during walking can be seen in the analysis of muscle synergies, which is similar to the concept of kinematic synergy. Groups of simultaneously active muscles and their activation patterns have been investigated as muscle synergies (Tresch et al. 1999; d'Avella et al. 2003; Hagio and Kouzaki 2014; Nishida et al. 2017; Kubo et al. 2017; Kibushi et al. 2018). During walking, sets of extracted muscle synergies have been used to characterize muscle patterns that are related to walking subtasks (e.g., loading response, forward propulsion, or swing leg) (Neptune et al. 2009; McGowan et al. 2010; Allen and Neptune 2012). When walking speeds change, major changes in muscle synergies are observed in the temporal patterns of muscle synergies. Although muscle synergy constructions were similar across walking speeds, temporal patterns of muscle synergies were dependent on walking speeds (Kibushi et al. 2018). This finding implies that the temporal pattern reflects the demand of kinematic output during walking. While the relationships between muscle synergies and kinematic synergies have not been revealed, both muscle synergies and kinematic synergies are associated with the walking subtasks. Therefore, we speculated that in addition to muscle synergies, temporal coordination of kinematic synergies also reflects the demand of kinematic output.

To investigate the characteristics of temporal coordination of kinematic synergies, we used the maximum Lyapunov exponents. The maximum Lyapunov exponent is one of the method for characterizing stability, and has been utilized in the fields of engineering, robotics, computer simulation, and experimental studies of walking (Bruijn et al. 2011, 2012; Huang et al. 2014, 2017; Dingwell and Marin 2006; Dingwell and Kang 2007; Kang and Dingwell 2008; Lockhart and Liu 2008; England and Granata 2007). The maximum Lyapunov exponent quantifies how the system responds to small internal perturbations (Bruijn et al. 2009; Santuz et al. 2018), and the local dynamic stability is quantified by the maximum Lyapunov exponents (Dingwell and Kang 2007). The local dynamic stability during various walking speeds or stride time–length combinations has been revealed (England and Granata 2007; Dingwell and Marin 2006; Hak et al. 2013). In these studies, maximum Lyapunov exponents were calculated using joint angle, variability of trunk motion or pelvis motion. However, how the stride time–length combination affects local dynamic stability in the temporal coordination of kinematic synergies has not been investigated. One merit in analysis of kinematic synergies is that we can evaluate segment mechanics as different coordination patterns that relate to subtasks within a gait cycle. Therefore, investigating the maximum Lyapunov exponents in the temporal coordination of kinematic synergies might contribute to characterizing the stability related to whole body kinematic coordination. We speculated that changes of local dynamic stability depending on the stride time–length combination are different among kinematic synergies. Then, we considered that characterizing the local dynamic stability in temporal coordination of kinematic synergies by the maximum Lyapunov exponents is needed.

In this study, we calculated the maximum Lyapunov exponents in temporal coordination of kinematic synergies to quantify time series characteristics in temporal coordination. We hypothesized that the maximum Lyapunov exponents of temporal coordination would depend on stride time–length combinations. The purpose of this study was to identify local dynamic stability of temporal coordination among different stride time–length combinations.

Methods

Subjects

Ten healthy men participated in this study (age 25 ± 2.6 years, height 171.2 ± 2.23 cm, weight 66 ± 3.9 kg). The subjects provided written informed consent to participate in the study after receiving a detailed explanation of the purpose, potential benefits, and risks associated with participation. The experimental procedures were conducted in accordance with the Declaration of Helsinki and were approved by the

Local Ethics Committee of the Graduate School of Human and Environmental Studies, of Kyoto University.

Experimental setup

Subjects walked at three non-dimensional walking speeds (0.15, 0.4, and 0.7: slow, middle, and fast walking speeds) with five types of stride length (very short, short, preferred, long and very long) in a random order. They walked on the treadmill over 160 gait cycles at each stride time–length combinations. Non-dimensional speed were defined as $v^* = v/\sqrt{gL_{\mathrm{leg}}}$, where v^* is the non-dimensional speed, v is the absolute walking speed, g is the gravitational acceleration, and L_{leg} is the subject's leg length (Snaterse et al. 2011; Vaughan et al. 2003; Liu et al. 2008). In addition, the non-dimensional stride time was also calculated as $t^* = t/\sqrt{g/L_{\mathrm{leg}}}$, where t^* is the non-dimensional speed, and t is the absolute stride length (Snaterse et al. 2011). During preferred stride length conditions, subjects selected a comfortable stride length combination for a given walking speed. In the conditions of the very short and very long stride length, we asked subjects to walk with as small/large of a stride length as possible. During short and long stride length conditions, subjects adjusted to the desired stride time–length combinations. The desired non-dimensional stride times of slow-short, slow-long, middle-short, middle-long, fast-short, and fast-long were 0.3, 0.9, 0.27, 0.4, 0.2, and 0.27, respectively. These values were determined based on preliminary experiments. To adjust to the desired stride time–length combinations, visual feedback of the current stride time–length combinations was given to subjects via Labview (NI USB-6229 BNC, National Instruments, Austin, TX, USA; Fig. 1). Subjects wore shoes equipped with a force-sensing register (FSR402, Interlink Electronics, California, USA) to detect heel contact timing. While subjects were given the visual feedback, we calculated stride times with Labview using the timings of the heel contacts that were derived from the force-sensing resistor. One gait cycle was defined as the time between the initial right heel contact and the moment before the next right heel contact. For the short and long stride length conditions, we instructed subjects to adjust the visualized stride time–length combination point (Fig. 1 light blue circle) to the target point (Fig. 1 white circle). We also provided information about the current absolute stride time (s) and stride length (m) to motivate subjects during the very long and very short stride length conditions.

Kinematic data were recorded with a three-dimensional optical motion capture system with 18 cameras operating at 100 Hz (Optotrak®, Northern Digital Inc., Waterloo, Ontario). This system captured three-dimensional coordinates of reflective markers that were attached to anatomical landmarks on the subjects. These reflective markers that were attached to the subjects were positioned at the top right and left side of the heads, as well as on the acromions, elbows, wrists, anterior superior iliac spines, posterior superior iliac spines, greater trochanters, medial and lateral epicondyles, medial and lateral

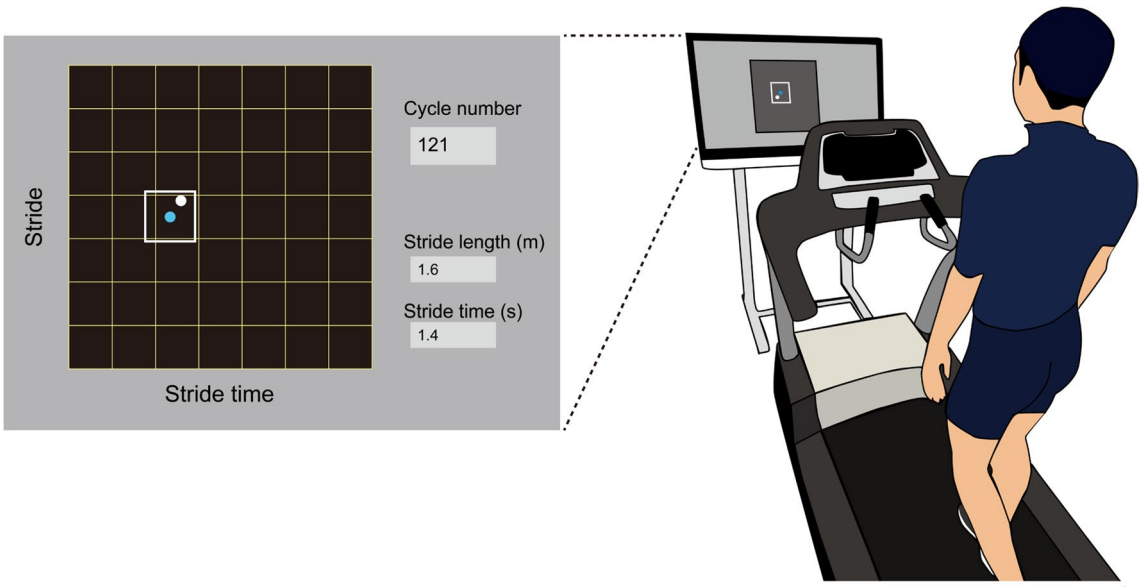

Fig. 1 Experimental setup. Subjects walked on the treadmill for over 150 gait cycles. Visual feedback of the current stride time–length combination was provided using Labview to adjust to the desired stride time–length combinations. An illustration of the visual feedback is presented in the left panel. During walking, current stride time, stride length and gait cycle number were also presented in the panel

malleolus, heels and toes. The measured reflective marker data were low-pass filtered at 10 Hz (Kang and Dingwell 2008).

Extraction of kinematic synergies

We calculated seven elevation angles (right-foot, right-shank, right-thigh, trunk, left-thigh, left-shank, and left-foot segment) to extract the kinematic synergies. Our selection of elevation angles was based on the assumption that changes in elevation angles are more stereotypical than relative angles (Borghese et al. 1996; Ivanenko et al. 2007). The elevation angles were calculated for 100 gait cycles without time normalization. To prepare to extract kinematic synergies, mean postures were computed by averaging the elevation angles over a time course of 100 gait cycles for each segment angle and stride time–length combination (Funato et al. 2010, 2015). We constructed a processed elevation angle matrix ($\Theta^{7\times t}$; t is the sample size for 100 gait cycles) for the extraction of kinematic synergies by subtracting the mean postures from elevation angles. The kinematic synergies were extracted from the processed elevation angle matrix by singular value decomposition (SVD) (Funato et al. 2010, 2015; Sano and Wada 2017). By applying SVD to the processed elevation angle matrix, the processed elevation angle matrix was decomposed into the intersegmental coordination z_i and the temporal coordination $\left(\lambda_i v_i\right)^T$,

$$\Theta = \sum_{i=1}^{N} z_i \left(\lambda_i v_i\right)^T. \quad (1)$$

Intersegmental coordination represents the principal groups of the simultaneously active joint group in the ith kinematic synergy, and the temporal coordination indicates activation patterns of ith kinematic synergy.

The number of kinematic synergies was determined based on the cumulative contribution ratio (Funato et al. 2010, 2015; Sano and Wada 2017). The cumulative ratios were calculated as $\sum_{i=1}^{j} \lambda_i^2 / \sum_{i=1}^{7} \lambda_i^2$. In this study, almost all cumulative contribution ratios exceeded 85% if the number of kinematic synergies was over 4 (Fig. 2). This finding implies that more than 85% of the processed elevation angle data can be characterized by these four kinematic synergies. Therefore, we determined the number of kinematic synergies to be 4.

Calculation of maximum Lyapunov exponents

We calculated the maximum Lyapunov exponent of the temporal coordination. For calculation of the maximum Lyapunov exponents, we selected a time-delayed coordinate approach (Dingwell and Marin 2006; Dingwell and Kang 2007; Dingwell and Cusumano 2000; Labini et al. 2012). In construction of the time-delayed coordinate system, the state space was constructed from single-dimensional time series measurements and its time delayed copies. The number of data points were ranged from 3000 to 27,582; this different number of data point was derived from different times for achieving 100 gait cycles among conditions and subjects. The time-delayed coordinate system of the temporal

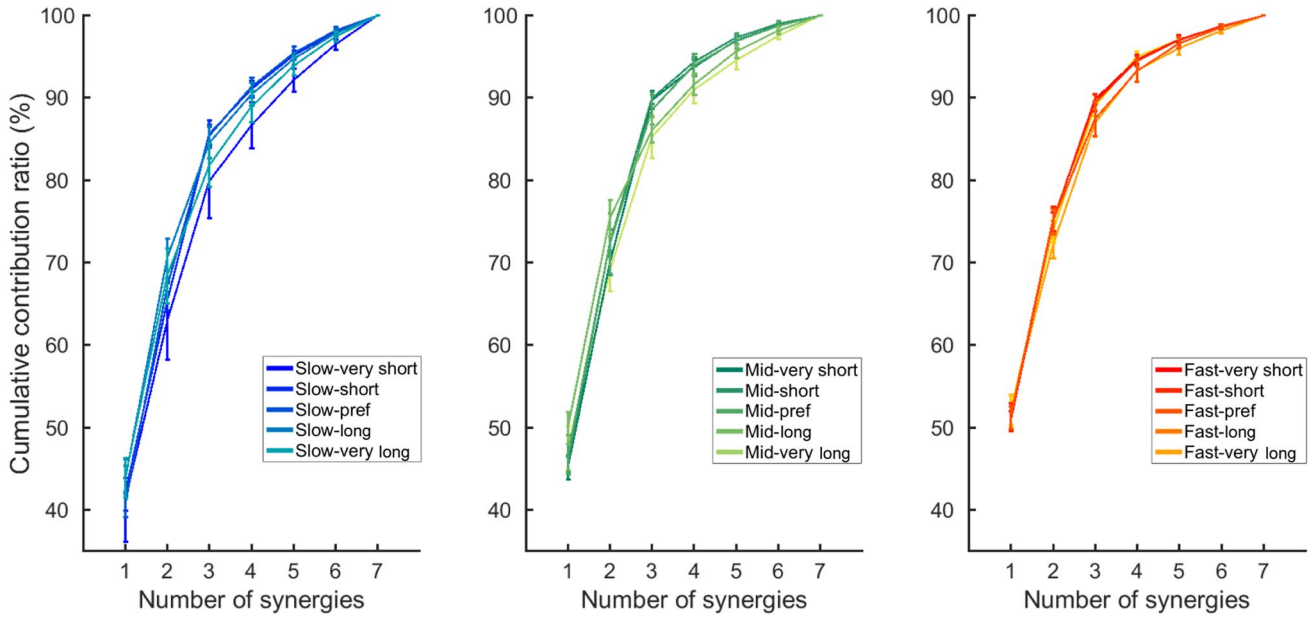

Fig. 2 Average cumulative contribution ratio across subjects. Average cumulative contribution ratios are presented as lines. Vertical lines on the average cumulative contribution ratios denote the standard deviations

coordination was constructed for each stride time–length combination. The general form of the state space is

$$S(t) = \left[q(t),\ q(t+\tau), \ldots, q\left(t+\left(d_{\mathrm{E}}-1\right)\tau\right)\right], \quad (2)$$

where $S(t)$ is the state space, $q(t)$ denotes the original single-dimensional data, τ is the selected time delay, and d_{E} is the embedding dimension. Based on the assumption that the embedding dimension should be unified among subjects (van Schooten et al. 2013), we unified the embedding dimension. The appropriate embedding dimension for each measurement was searched for by Global False Nearest Neighbor (FNN) analysis (Kennel et al. 1992). When the number of false neighbors on the reconstructed trajectory was minimized, the appropriate embedding dimension was determined. The calculated embedding dimensions were averaged across subjects, stride time–length combination, and temporal coordination. From these procedures, the unified embedding dimension was computed as 4. We determined time delays by calculating the first minimum of the average mutual information function (Fraser and Swinney 1986). The time delays of the temporal coordination were 0.23 ± 0.025, 0.23 ± 0.036, 0.24 ± 0.026, and 0.28 ± 0.055 (s). The average exponential rate of divergence of the neighboring trajectories in the state space was quantified by the maximum Lyapunov exponents (Rosenstein et al. 1993). We calculated Euclidean distances between a point in a state space and its nearest neighbor. This computation was repeated for all data points in the state spaces. The divergence was calculated as a function of time,

$$\lambda(i) = \left\langle \ln\left[D_j(i)\right]\right\rangle / \Delta t, \quad (3)$$

where $D_j(i)$ is the Euclidean distance between the jth pair of nearest neighbors after the i discrete time steps, Δt is the sampling period of the time series data, and $\langle \cdots \rangle$ denotes the average over all values of j. Maximum Lyapunov exponents were estimated from the slopes of linear fits to the curve. We defined the maximum Lyapunov exponent from the slopes of linear fits to the divergence curve between 0 and 1 strides (Dingwell and Marin 2006). The maximum Lyapunov exponent is negative if distances among trajectories of an attractor converge. On the other hand, the maximum Lyapunov exponent is positive if distances among trajectories of an attractor diverge.

Statistics

A one-way ANOVA for repeated measures was applied to investigate the effect of walking speed or stride length on the maximum Lyapunov exponents in the temporal coordination of kinematic synergies.

Results

Characteristics of gait parameter and elevation angles

Walking speed, stride time and stride length are presented in Table 1. During the short and long stride length conditions the standard deviations were small, indicating that subjects appropriately adjusted to the desired stride time–length combinations. We calculated elevation angle of each segment during walking. Average elevation angles are illustrated in Fig. 3. Peak amplitudes of the elevation angles became large as walking speeds increased. In addition, peak amplitudes of the elevation angles increased as stride length were extended. The behavior of each elevation angle within one gait cycle was also affected by walking speeds and the stride time–length combinations. The elevation angles of the foot

Table 1 Average walking speeds, stride time, and stride length across subjects

	Very short	Short	Preferred	Long	Very long
Slow walking speed					
Speed (m/s)	0.44 ± 0				
Time (s)	0.48 ± 0.115	0.98 ± 0.013	1.82 ± 0.396	2.95 ± 0.032	4.36 ± 0.628
Length (m)	0.21 ± 0.051	0.44 ± 0.006	0.81 ± 0.176	1.31 ± 0.014	1.94 ± 0.279
Middle walking speed					
Speed (m/s)	1.20 ± 0.016				
Time (s)	0.50 ± 0.101	0.89 ± 0.012	1.14 ± 0.048	1.30 ± 0.020	1.70 ± 0.202
Length (m)	0.60 ± 0.125	1.06 ± 0.006	1.36 ± 0.058	1.56 ± 0.027	2.03 ± 0.235
Fast walking speed					
Speed (m/s)	2.09 ± 0.019				
Time (s)	0.53 ± 0.083	0.65 ± 0.017	0.84 ± 0.047	0.88 ± 0.017	1.01 ± 0.110
Length (m)	1.10 ± 0.176	1.37 ± 0.029	1.76 ± 0.098	1.85 ± 0.024	2.11 ± 0.236

In the slow walking speeds, all subjects walked at 0.44 m/s. Therefore, the standard deviation of the slow walking speeds was 0

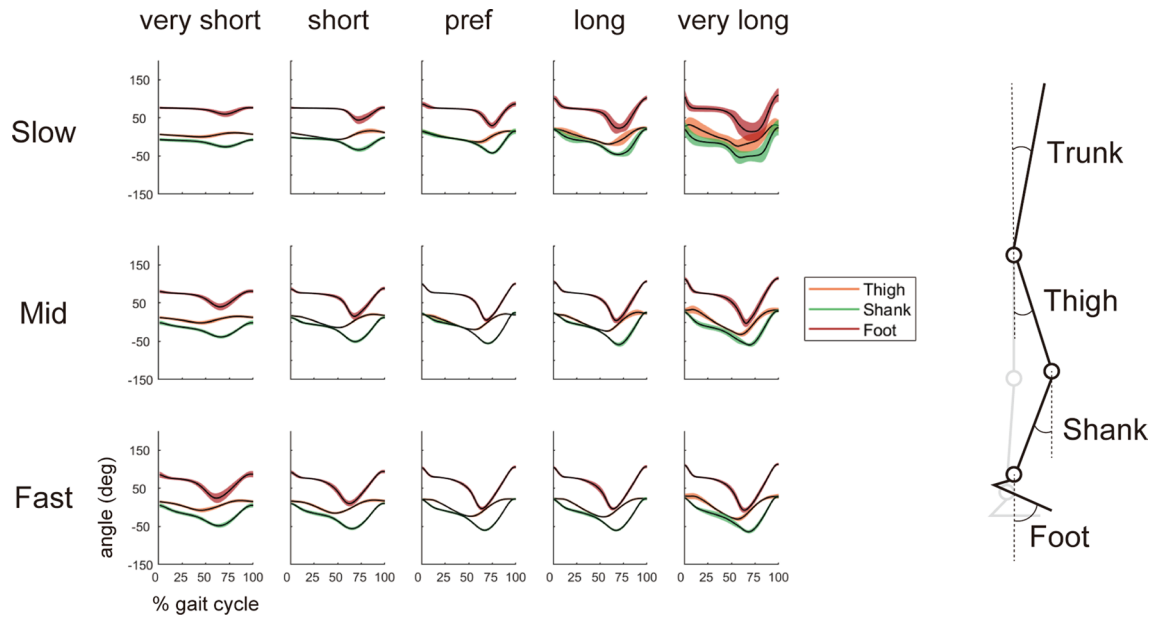

Fig. 3 Average elevation angles across subjects. Average elevation angles of the right thigh, shank, and foot are presented in each plot. To display average temporal patterns, we time-normalized elevation angles. Black lines indicate the average elevation angles, and shaded areas denote the standard deviation of the elevation angles. The definition of the elevation angle is illustrated on the right side of the figure, where each black dashed line is a perpendicular line from a joint. An elevation angle is positive if a segment is located ahead of a perpendicular line. On the other hand, an elevation angle is negative if a segment is located behind a perpendicular line

segment within one gait cycle were highest between the moment before heel contact and heel contact to perform ankle dorsiflexion. This ankle dorsiflexion became large as walking speeds and stride length increased. Elevation angles of the foot segment were lowest during the swing phase. For the very short stride length, changes in the elevation angle of the shank and thigh segments were small. On the other hand, amplitudes of the elevation angle of the shank and thigh segments were large in the very long stride length condition. Contrary to foot, shank, and thigh segments, changes of the elevation angle of trunk were small across the stride time–length combinations.

Extracted kinematic synergies

We extracted four kinematic synergies from the elevation angle matrix (Figs. 4, 5). Because elevation angles contain both positive and negative values, intersegmental coordination and temporal coordination also contain both positive and negative value. Intersegmental coordination represents the spatial pattern, and temporal coordination represents the temporal pattern in the kinematic synergies. A positive intersegmental coordination value means the major axis of segment is located in front of a vertical line from a joint. Conversely, a negative intersegmental coordination value indicates that the major axis of the segment is located behind a vertical line from a joint. The temporal coordination determines when and how the spatial pattern that is constructed by intersegmental coordination activate. In the case of positive temporal coordination, the sign of intersegmental coordination does not exchange. In the case of negative temporal coordination, the sign of intersegmental coordination does exchange. The intersegmental coordination of Synergy 1 was mainly constructed by both sides of the foot and shank segments, and Synergy 1 was activated during the swing phase. Synergy 1 was related to alternating the lower limbs back and forth (Fig. 5: Synergy 1). The amplitude of the temporal coordination of Synergy 1 became large as stride length increased. The construction of the intersegmental coordination of Synergy 2 was similar to that of Synergy 1; specifically, both sides of the foot and shank segments mainly constructed the intersegmental coordination of Synergy 2. In the intersegmental coordination of Synergy 1, the left shank and thigh were positive. However, the left shank and foot were negative in the intersegmental coordination of Synergy 2. This finding indicates that Synergy 2 contributed to the motion of synchronously moving the lower limbs (Fig. 5: Synergy 2). The timing of the positive peak of the temporal coordination in Synergy 2 was located around the pre-swing phase. The amplitude of the temporal coordination became large as stride length was extended. Both sides of the thigh primarily dominated the intersegmental coordination of Synergy 3 and Synergy 4, and both sides of the thigh segment in Synergy 4 were positive. However, the right thigh was negative in the Synergy 3. The negative peak amplitude of the temporal coordination of Synergy 3 was located around the

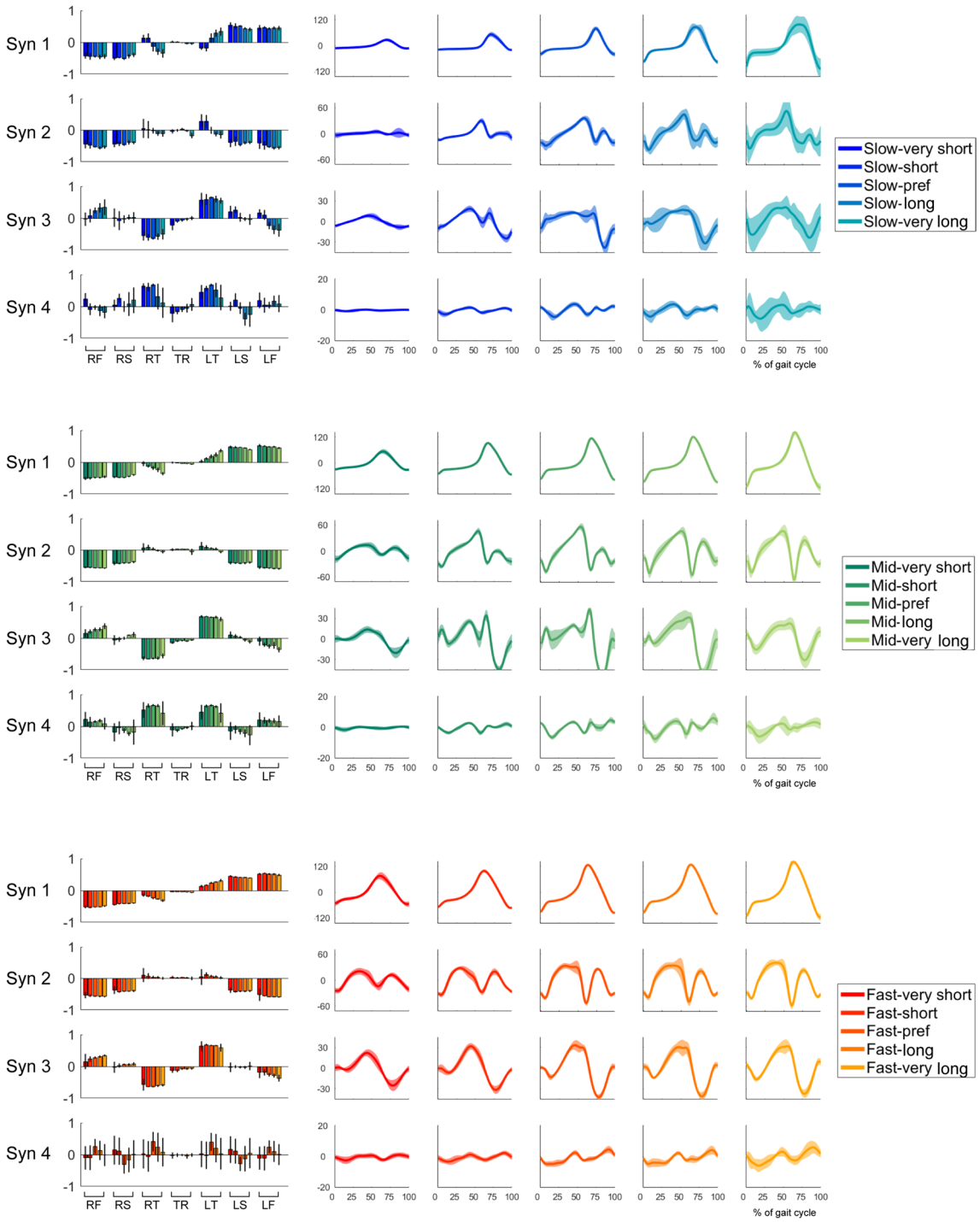

Fig. 4 Average kinematic synergies across subjects. Bars represent intersegmental coordination and wave forms indicate temporal coordination. To display average temporal patterns, we time-normalized temporal patterns of kinematic synergies. Standard deviations for intersegmental coordination and temporal coordination are indicated as black lines and shaded areas, respectively. The results for each walking speed are located in the upper (slow speed), middle (middle speed), and lower (fast speed) rows. Abbreviations represent the elevation angle of right foot (RF), right shank (RS), right thigh (RT), trunk (TR), left thigh (LT), left shank (LS), and left foot (LF)

mid-swing phase. Synergy 3 was associated with exchanging the thigh segments back and forth (Fig. 5: Synergy 3). The amplitude of the temporal coordination of Synergy 4 was relatively small, and Synergy 4 contributed to synchronously moving the thigh segments (Fig. 5: Synergy 4). To investigate how kinematic synergies were affected by stride

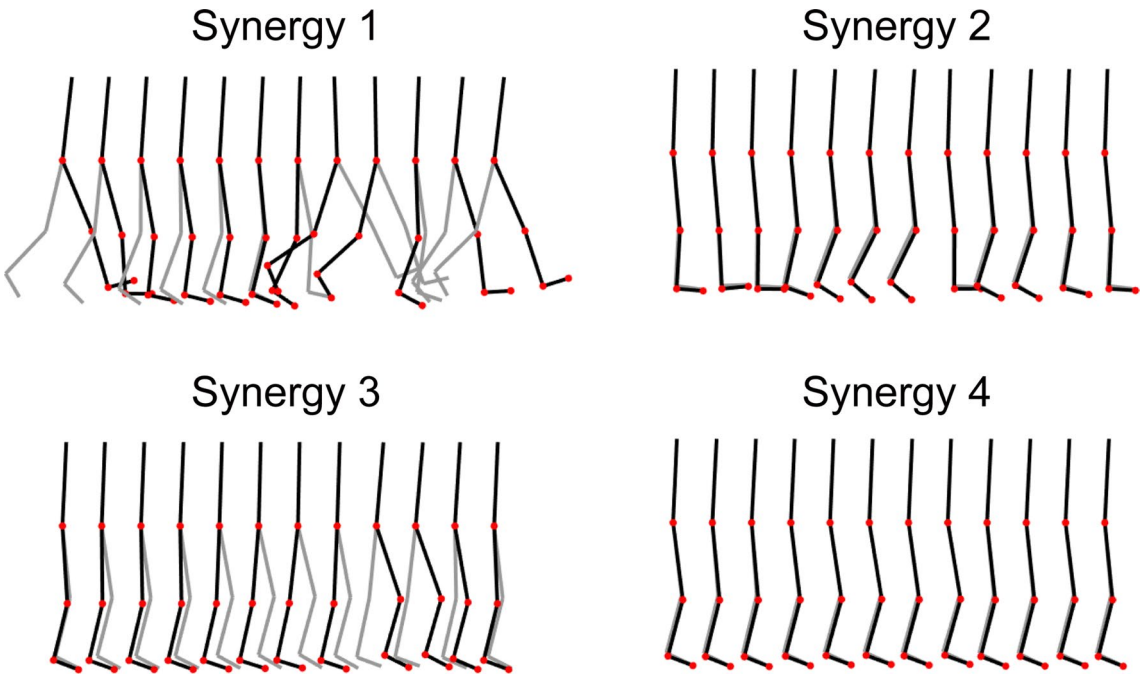

Fig. 5 Illustration of function of kinematic synergies in a representative subject during middle walking speed with preferred stride length. To describe the function of kinematic synergies clearly, we provided illustrations of motions reconstructed from each kinematic synergy. In producing stick pictures, we reconstructed elevation angles from each kinematic synergy. The hip joint position was set as the origin, and other joint positions were calculated using elevation angles and trigonometric functions. The stride length in the stick pictures was intentionally set widely to display the motion clearly

time–length combinations, we calculated similarities of kinematic synergies between middle walking speed with preferred stride length and other stride time–length combinations (Fig. 6). The intersegmental coordination was similar among stride time–length combinations except for Synergy 4. On the other hand, the temporal coordination was changed by the stride time–length combinations except for Synergy 1. Especially, temporal coordination in the fast walking speeds and very short stride length conditions was different from middle walking speed with preferred stride length.

The maximum Lyapunov exponents of temporal coordination

The maximum Lyapunov exponents of temporal coordination are shown in Fig. 7 and Table 3. All maximum Lyapunov exponents were positive, indicating that the local dynamic stability of temporal coordination is unstable. The maximum Lyapunov exponents were influenced by the stride time–length combinations. Therefore, our expectation that the maximum Lyapunov exponents of temporal coordination depend on stride time–length combinations were supported by the results of this study. In all kinematic synergies, the maximum Lyapunov exponents were high at fast walking speeds and very short stride length conditions. Conversely, the maximum Lyapunov exponents were small at slow and very long stride conditions. This result implies that fast walking speeds and very short stride lengths are associated with lower local dynamic stability in the temporal coordination, and slow-very long strides contributed to low instability. We also found that the characteristics of the contour plots of maximum Lyapunov exponents were locally different among the kinematic synergies. In Synergy 1, which was related to exchanging lower limbs back and forth, the maximum Lyapunov exponents of temporal coordination increased with acceleration of walking speeds within the same stride length conditions. Although the maximum Lyapunov exponents decreased as stride length were extended at the slow and middle walking speeds ($p < 0.001$: Table 2), high maximum Lyapunov exponents were relatively constant at the fast walking speed. The changes of maximum Lyapunov exponents of temporal coordination in Synergy 2 were complicated. Synergy 2 was mainly activated around the pre-swing phase and the maximum Lyapunov exponents of temporal coordination in Synergy 2 during slow walking speeds decreased as stride length were extended. Although the difference was not clear, the maximum Lyapunov exponents in Synergy 2 during the middle walking speed were maximized at the preferred stride time–length combination. Contrary to the middle walking speed, the maximum Lyapunov exponents during fast walking speeds were minimized around the preferred stride

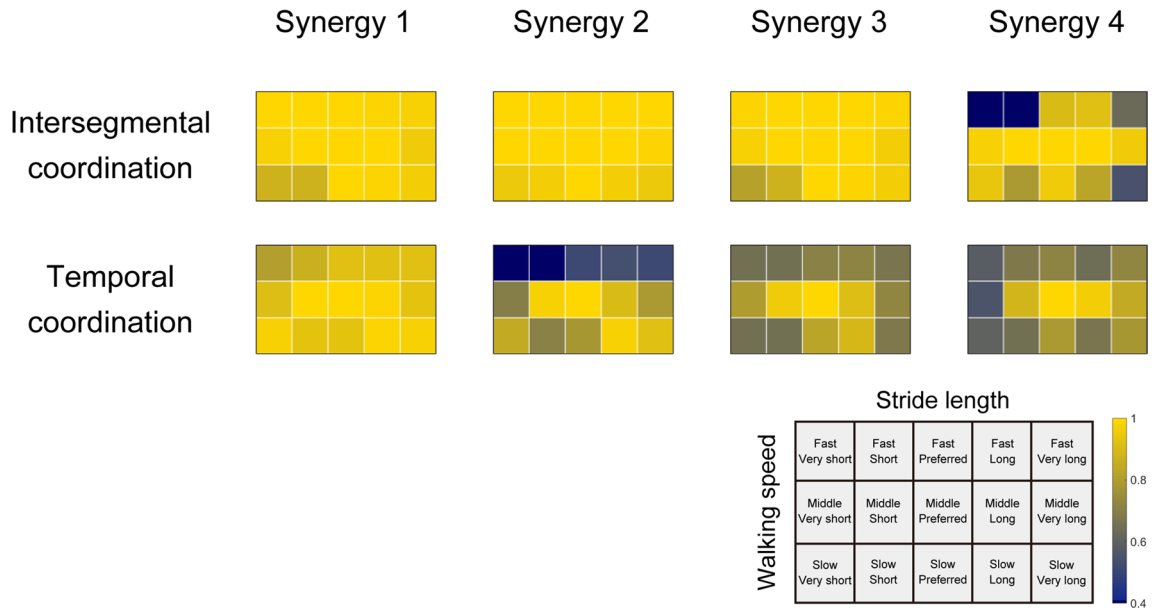

Fig. 6 Similarities of kinematic synergies among stride time–length combinations. We used the cosine similarity to evaluate similarities between the middle walking speed with preferred stride length and other conditions (Kibushi et al. 2018; Hagio et al. 2015). We calculated cosine similarities in average intersegmental coordination and temporal coordination between the middle walking speed with preferred stride length and other conditions. The extent of similarities was represented using colors. Blue color indicates relatively low similarity, and yellow color represents high similarity

length. In Synergy 3, which was associated with exchanging the thigh segments back and forth, the maximum Lyapunov exponents of temporal coordination decreased as stride length was extended during the slow walking speed ($p < 0.001$: Table 2). The maximum Lyapunov exponents were minimized around the preferred stride length at the middle and fast walking speeds. During the slow walking speed, the maximum Lyapunov exponents of temporal coordination in Synergy 4 decreased with extension of stride length ($p < 0.001$: Table 2). Synergy 4 was related to synchronously moving the thigh segments. Similar to the findings at the slow walking speeds, the maximum Lyapunov exponents of temporal coordination in Synergy 4 decreased with extension of stride length for the middle and fast walking speeds. However, the maximum Lyapunov exponents of temporal coordination were slightly minimized around the preferred stride length in Synergy 4 during the middle and fast walking speeds (Table 3).

Discussion

The purpose of this study was to identify time series characteristics in temporal coordination across various stride time–length combinations by analysis of the maximum Lyapunov exponents that represent the local dynamic stability. We extracted four kinematic synergies and calculated the maximum Lyapunov exponents of temporal coordination for the various stride time–length combinations. It was determined that the stride time–length combinations affected the maximum Lyapunov exponents of temporal coordination. Moreover, the maximum Lyapunov exponents were high at fast walking speeds and very short stride length conditions. Conversely, the maximum Lyapunov exponents were small at slow-very long stride conditions. This finding implies that fast walking speeds and very short stride lengths were associated with lower local dynamic stability in the temporal coordination, and slow-very long strides contributed to low instability. We considered that kinetic or kinematic outputs that depend on the stride time–length combinations might affect the maximum Lyapunov exponents of temporal coordination. Therefore, subsequently we discuss the stride time–length combination dependent factors (e.g., kinetics or kinematics) that may affect the maximum Lyapunov exponents of temporal coordination. In addition, we found a difference in changes in the local minimum point of maximum Lyapunov exponents around the preferred stride length in temporal coordination. This is discussed in the final section.

Relationships between high maximum Lyapunov exponents and kinetic or kinematic characteristics of fast walking speeds and very short stride length

In this study, we revealed that the maximum Lyapunov exponents were high for fast walking speeds and very short stride length conditions (Fig. 7). This finding implies that

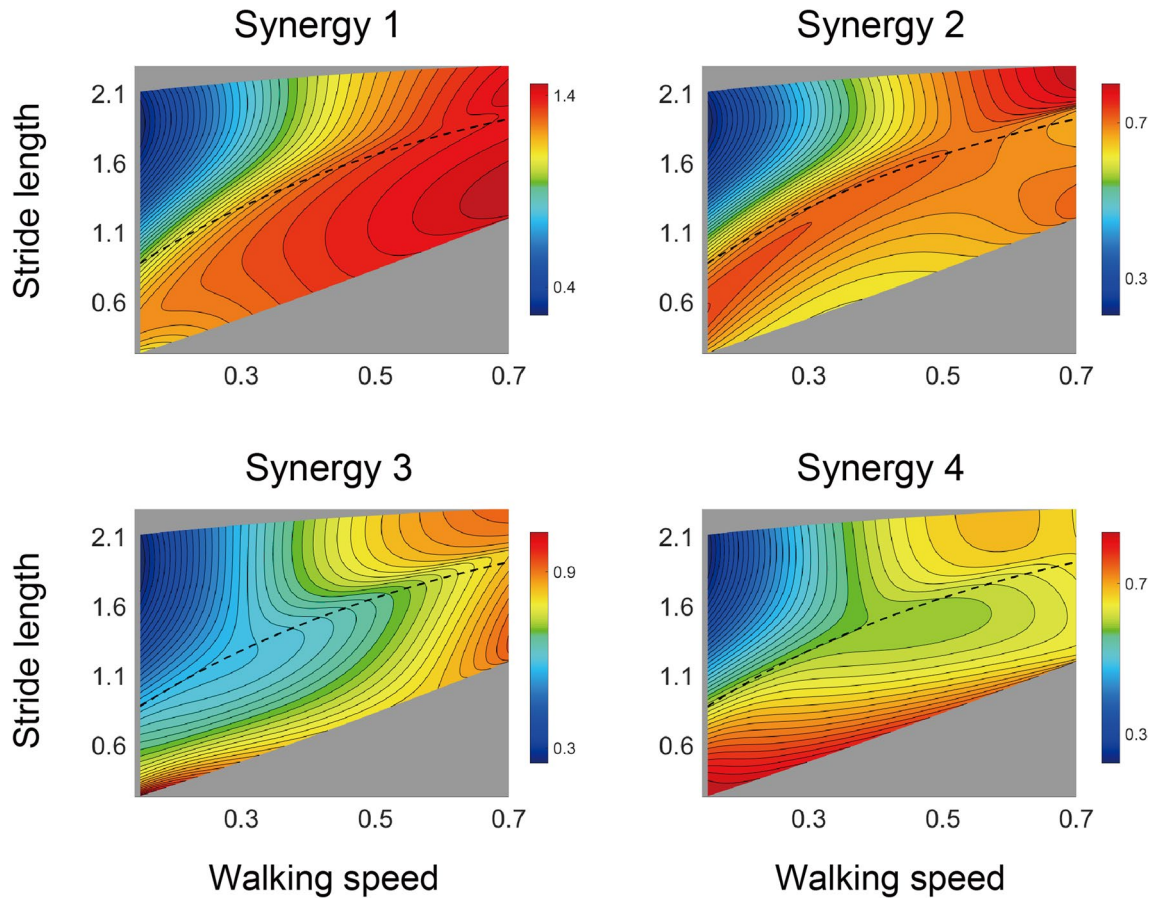

Fig. 7 The contour plots of maximum Lyapunov exponents of temporal coordination. To create contour plots, average maximum Lyapunov exponents across subjects, stride length, and walking speeds were interpolated. High maximum Lyapunov exponents are illustrated as a warm color, and low maximum Lyapunov exponents are illustrated as a cold color. The stride length-walking speed plane of the contour plots of maximum Lyapunov exponents is presented. Black dashed lines denote the average preferred stride length

fast walking is associated with lower instability in the dynamical system. We considered "fast walking" as walking at a fast speed or very short stride lengths. These fast walking speeds and very short stride lengths might cause high maximum Lyapunov exponents of temporal coordination. Increased maximum Lyapunov exponents with acceleration of walking speeds have been reported in the joint angle or variability of trunk motion (England and Granata 2007; Dingwell and Marin 2006). In this study, we also found maximum Lyapunov exponents of temporal coordination increased with acceleration of walking speeds. This indicates that both local dynamic stability in individual kinematic outputs (e.g., joint angle or trunk motion) and local dynamic stability in temporal coordination are affected by walking speeds. In addition, changes of local dynamic stability in temporal coordination are also affected by the stride length. However, some researches did not correspond to our results. It has been reported that the local dynamic stability of pelvis motion was not affected by the stride time–length combinations and walking speed (Hak et al. 2013). In addition, McAndrew et al. (2012) revealed that the short-term maximum Lyapunov exponents of trunk motion were significantly high in long step length. These results seemed not to correspond to our results. Now, we discuss two points which did not correspond to previous studies. First, we discuss the difference about relationships between walking speed and local dynamic stability. Dingwell and Marin (2006) revealed that the short-term Lyapunov exponents of trunk variability increased with acceleration of walking speed. Other researches (Dingwell et al. 2000; England and Granata 2007; Kang and Dingwell 2008) and our results were similar to Dingwell and Marin (2006). In contrast, Hak et al. (2013) proposed that the short-term Lyapunov exponents of trunk motion were not affected by walking speeds. This might be derived from different state spaces. Dingwell and Marin (2006) and we constructed state spaces from time-delayed copies of single vector (single-dimensional trunk motion or single temporal coordination). On the other hand, Hak et al. (2013) constructed state spaces from time-delayed copies

Table 2 Results for F values and p values obtained by one-way ANOVA

Walking speed	F	p	Stride condition	F	p
Synergy 1					
Slow	55.78	< 0.001	Very short	4.54	0.02
Middle	11.18	< 0.001	Short	9.87	0.001
Fast	0.42	0.792	Preferred	20.04	< 0.001
			Long	169.2	< 0.001
			Very long	204.6	< 0.001
Synergy 2					
Slow	42.17	< 0.001	Very short	0.33	0.721
Middle	1.23	0.312	Short	0.790	0.464
Fast	2.52	0.054	Preferred	1.24	0.306
			Long	87.36	< 0.001
			Very long	220.6	< 0.001
Synergy 3					
Slow	39.70	< 0.001	Very short	1.40	0.264
Middle	1.46	0.220	Short	22.14	< 0.001
Fast	0.78	0.543	Preferred	18.23	< 0.001
			Long	35.43	< 0.001
			Very long	110.3	< 0.001
Synergy 4					
Slow	57.49	< 0.001	Very short	0.726	0.494
Middle	2.47	0.058	Short	9.76	0.001
Fast	0.43	0.785	Preferred	1.33	0.281
			Long	64.25	< 0.001
			Very long	97.20	< 0.001

A one-way ANOVA for repeated measures was applied to investigate the effect of walking speed or stride length on the maximum Lyapunov exponents in temporal coordination of kinematic synergies

The F values are indicated as F, and the p values are represented as p

Table 3 The average maximum Lyapunov exponent values among subjects and their standard deviations

SL/WS	Slow	Middle	Fast
Synergy 1			
Very short	1.08 ± 0.288	1.31 ± 0.214	1.38 ± 0.181
Short	1.21 ± 0.132	1.33 ± 0.123	1.45 ± 0.110
Preferred	0.99 ± 0.183	1.25 ± 0.068	1.38 ± 0.145
Long	0.44 ± 0.041	1.09 ± 0.105	1.41 ± 0.172
Very long	0.31 ± 0.074	0.99 ± 0.135	1.38 ± 0.125
Synergy 2			
Very short	0.64 ± 0.178	0.61 ± 0.272	0.69 ± 0.170
Short	0.72 ± 0.051	0.68 ± 0.072	0.69 ± 0.107
Preferred	0.65 ± 0.122	0.70 ± 0.056	0.66 ± 0.048
Long	0.33 ± 0.043	0.62 ± 0.047	0.73 ± 0.101
Very long	0.24 ± 0.059	0.59 ± 0.042	0.80 ± 0.071
Synergy 3			
Very short	1.04 ± 0.305	0.81 ± 0.375	0.88 ± 0.179
Short	0.73 ± 0.104	0.64 ± 0.076	0.91 ± 0.094
Preferred	0.58 ± 0.085	0.62 ± 0.089	0.83 ± 0.122
Long	0.34 ± 0.060	0.69 ± 0.158	0.84 ± 0.167
Very long	0.26 ± 0.060	0.72 ± 0.101	0.92 ± 0.119
Synergy 4			
Very short	0.84 ± 0.166	0.78 ± 0.323	0.70 ± 0.226
Short	0.78 ± 0.113	0.62 ± 0.082	0.63 ± 0.083
Preferred	0.60 ± 0.122	0.58 ± 0.085	0.65 ± 0.072
Long	0.34 ± 0.042	0.59 ± 0.082	0.66 ± 0.072
Very long	0.23 ± 0.049	0.61 ± 0.089	0.65 ± 0.072

We calculated the maximum Lyapunov exponents in the temporal coordination. Although the contour plots easily represent how the maximum Lyapunov exponents were changed by different conditions, we cannot represent the variability of maximum Lyapunov exponents. Thus, this table indicates the variability of maximum Lyapunov exponents among subjects

of three-dimensional vector of trunk motion. Therefore, analyzed state spaces were different between our research and Hak et al. (2013), and these different state spaces might influence on the different results about relationships between walking speed and local dynamic stability. Second, we discuss the difference about relationships between the stride/step length and local dynamic stability. McAndrew et al. (2012) revealed that the short-term maximum Lyapunov exponents of trunk motion were significantly high in long step length. This seemed not to correspond to our results, because our results indicated that the maximum Lyapunov exponents were decreased with extending the stride length. We suggested that differences might be caused by small contribution of trunk in our extracted kinematic synergies. We found that weightings of intersegmental coordination of trunk were extremely small, because range of elevation angle of trunk was smaller than the other elevation angles. Different results about relationships between step length and local dynamic stability might be caused by small contribution of trunk in the present study.

In addition to the results of McAndrew et al. (2012) and Hak et al. (2013), revealed stride length/frequency did not influence on the short-term Lyapunov exponents. As we described in the previous, constructed state spaces were different between our research and Hak et al. (2013); different changes of local dynamic stability might be caused by different state spaces. Moreover, ranges of stride length and stride time were extremely wide in our research. For example, our results of stride length in middle walking speed ranged from 44.1 to 150% of preferred stride length, and stride time ranged from 43.9 to 150% of preferred stride time. In contrast, stride length and stride frequency in Hak et al. (2013) ranged from 84 to 119.1% of preferred stride length/frequency. Wide range of stride length/time in our study might contribute to significant changes in maximum Lyapunov exponents.

Synergies 1, 2, and 3 were associated with exchanging the lower limbs back and forth, synchronously moving lower

limbs, and exchanging the thigh segments back and forth, respectively. The highest peak temporal coordination of Synergies 1, 2, and 3 were observed during the swing phase. Therefore, Synergies 1–3 mainly contributed to leg swing. The maximum Lyapunov exponents of temporal coordination of Synergies 1–3 increased with acceleration of walking speeds within the same stride length condition (Fig. 7). These high maximum Lyapunov exponents of temporal coordination during fast walking speeds might be due to the fast leg swing motion. In the case of normal walking speed, effort required to swing the leg is small because the energy cost to swing the leg is small (Gottschall and Kram 2005). However, effort to swing leg increases in the case of fast walking speeds, and it has been reported that the metabolic work of swinging the legs is increased at high frequencies (Doke et al. 2005). Moreover, it was observed that activation of the hip flexor muscle (rectus femoris) during the swing phase in walking was higher than running when treadmill speeds were over the gait transition speed (Prilutsky and Gregor 2001). This finding indicates that muscle activity during the swing phase is exceedingly high in the case of fast walking speeds, which requires a large kinematic output to achieve the fast leg swing at fast walking speeds. This requirement of a large kinematic output might affect high maximum Lyapunov exponents of temporal coordination during fast walking speeds. In Synergy 4, the main peak of temporal coordination was located in the stance phase. Hence, Synergy 4 was associated with stance leg. It has been proposed that positive hip joint work during fast walking speeds is exceedingly high, and this high joint work during fast walking is larger than in slow running (Pires et al. 2014). This implies that hip joint work is high at fast walking speeds. As well as the fast swing leg, requirement for large output during stance phase might be related to the high maximum Lyapunov exponents of temporal coordination of Synergy 4.

To understand the unstable walking, we need to discuss the relationships between changes of kinematic synergies and unstable walking. A previous study connected the relationships between unstable walking and the concept of synergy and revealed high maximum Lyapunov exponents in spine motion under the unstable surface (Santuz et al. 2018) and reported a wider shape of activation of muscle synergies under the unstable surface. This finding means that the activations of muscle synergies were changed when achieving unstable walking. We also observed a difference in the temporal coordination among various conditions, and this difference was remarkable in very short stride length conditions and fast walking speeds. This may indicate that walking with fast walking speed and very short stride length is especially unstable whole body kinematic coordination.

Slow-very wide stride length was associated with small maximum Lyapunov exponents

The maximum Lyapunov exponents of temporal coordination in all kinematic synergies were small in slow-very long stride length conditions. This result indicates that slow-very long stride length resulted in small maximum Lyapunov exponents of temporal coordination. Previous studies have proposed a requirement of large output with extended stride length. For example, anteroposterior braking and propulsive forces increased as stride length was extended (Martin and Marsh 1992), and muscle work was also high with a long stride length (Lim et al. 2017). Therefore, we expected that the requirement of a large output in the very long stride length condition might affect the high maximum Lyapunov exponents of temporal coordination. However, the maximum Lyapunov exponents of temporal coordination in the slow-very long stride length condition were small (Fig. 7). Hence, small maximum Lyapunov exponents of temporal coordination might depend on other factors. During slow-very long stride length condition, subjects walked for at least over 9 min. In contrast, the walking tasks were completed in less than 90 s in the very short stride conditions. The slow-very long stride length condition may have advantages in terms of the sustainability of walking. To minimize maximum Lyapunov exponents of temporal coordination, the sustainability of walking might be a necessary factor.

The small maximum Lyapunov exponents of temporal coordination at slow speeds or with long stride lengths may provide useful clinical information. Reduction of walking speed has frequently been observed in elderly adults or individuals with disorders of the CNS (Lockhart and Liu 2008; Judge et al. 1996; Kerrigan et al. 1998; Clark et al. 2010; Balasubramanian et al. 2007; Steele et al. 2015). The slow walking speed that is frequently adopted in individuals with disorders of the CNS or elderly adults may reflect walking disabilities. However, it is possible that slow walking speeds may have advantages for the patients who have disorders of the CNS or elderly adults because the maximum Lyapunov exponents of temporal coordination are small at slow walking speeds. Further, it has been revealed that the maximum Lyapunov exponents of kinematic data in individuals with cerebellar ataxia (Hoogkamer et al. 2015), Parkinson's disease (Kurz et al. 2010), and a history of falls (Lockhart and Liu 2008) were higher than those of healthy or young adults. For these individuals, maximum Lyapunov exponents of the kinematics were high and were needed to avoid destabilization of walking. Hence, we supposed that one strategy for preventing destabilization of walking was to reduce walking speed. Because the maximum Lyapunov exponents were small at slow walking speeds, slow walking may be advantageous for the patients with disorders of the

CNS or elderly adults. In addition, extending stride length at slow walking speeds might help to prevent falls because extending stride length might contribute to small maximum Lyapunov exponents of temporal coordination. However, it has been shown that the elderly adults often reduce stride length (Elble et al. 1991), which may be related to high maximum Lyapunov exponents of temporal coordination. Thus, extending stride length might be an effective rehabilitation technique to decrease fall risk.

Local minimum point of maximum Lyapunov exponents around preferred stride length in middle and fast walking speeds

We found that the stride time–length combination affected the maximum Lyapunov exponents of temporal coordination. The changes of the maximum Lyapunov exponents varied across the kinematic synergies. Based on the evidence that the selection of the optimal stride time–length combinations or step width contributes to minimize energy cost (Bertram and Ruina 2001; Donelan et al. 2001; Kuo 2001), we expected that all the maximum Lyapunov exponents of temporal coordination would be minimized around the preferred stride length within the same walking speed. In Synergies 3 and 4, which were related to exchanging the thigh segments back and forth and synchronously moving the thigh segments, the maximum Lyapunov exponents were minimized around the preferred stride time–length combinations at the middle and fast walking speeds (Figs. 4, 7). However, the maximum Lyapunov exponents were not minimized around the preferred stride time–length combinations in Synergies 1 and 2, which were associated with exchanging the lower limb back and forth and synchronously moving the lower limb (Figs. 4, 7). This indicates that changes of local dynamic stability around preferred stride length and in middle and fast walking speeds are different among temporal coordination. This result might be caused by the difference in function of the kinematic synergies.

The maximum Lyapunov exponents of the temporal coordination in Synergy 3 were minimized around the preferred stride length at the middle and fast walking speeds (Figs. 4, 7), which might be related to the function of the Synergy 3. Synergy 3 contributed to exchanging the thigh segments back and forth, and this motion may be equivalent to the swing leg especially for the thigh segments. A previous study revealed that preferred ground clearance during the swing phase minimized the energy cost (Wu and Kuo 2016). Therefore, a preferred operation point exists for efficient swing leg. In addition to energy cost, the local dynamic stability of temporal coordination that related to swing leg might be minimized around the preferred stride length.

In Synergy 4, which was related to synchronously moving the thigh segments, the maximum Lyapunov exponents of temporal coordination decreased as stride length were extended within the same walking speeds (Fig. 7). However, the maximum Lyapunov exponents were slightly minimized around the preferred stride length for the middle and fast walking speeds. The amplitudes of temporal coordination in Synergy 4 were small within one gait cycle, and the largest amplitudes of temporal coordination were located in the mid-stance phase (Fig. 4). Therefore, Synergy 4 may contribute to single leg support. The minimized maximum Lyapunov exponents of temporal coordination in Synergy 4 might be related to the kinematics of single leg support. Lim et al. (2017) showed that the contribution of the hip abductor muscle (gluteus medius) to the vertical ground reaction force became small as stride time or length deviated from the preferred value. The gluteus medius muscle is mainly active during single leg support; hence the decreased contribution of the hip abductor muscle might result in an inefficient stance leg for un-preferred stride time–length combinations. Correspondingly, the inefficient stance leg might affect the high maximum Lyapunov exponents of temporal coordination in Synergy 4 for un-preferred stride time–length combinations.

Summary

In this study, we investigated the maximum Lyapunov exponents of temporal coordination among various stride time–length combinations to investigate time series characteristics in temporal patterns of kinematic synergies. We revealed that the maximum Lyapunov exponents of temporal coordination changed with the different stride time–length combinations. Moreover, the maximum Lyapunov exponents were high at fast walking speeds and very short stride length conditions. Therefore, we conclude that fast walking speeds and very short stride lengths are associated with lower local dynamic stability of temporal coordination.

Author contributions Conception and design of the experiments: BK, TM, and MK. Collection, analysis and interpretation of the data: BK. Drafting of the article or critical revision for important intellectual content: BK and MK. Final approval of the version to be published: BK, TM, and MK.

Funding This work was supported by the Grant-in-Aid for JSPS Research Fellow (Grant Number 16J07348); the Japanese Council for Science, Technology and Innovation (CSTI); and the Cross-ministerial Strategic Innovation Promotion Program (SIP Project ID 14533567 Funding agency: Bio-oriented Technology Research Advancement Institution, NARO).

Compliance with ethical standards

Conflict of interest The authors declare that they have no competing interests.

Data availability The datasets analyzed during the current study are available from the corresponding author on reasonable request.

References

Allen JL, Neptune RR (2012) Three-dimensional modular control of human walking. J Biomech 45(12):2157–2163

Balasubramanian CK, Bowden MG, Neptune RR, Kautz SA (2007) Relationship between step length asymmetry and walking performance in subjects with chronic hemiparesis. Arch Phys Med Rehabil 88(1):43–49

Bertram JE, Ruina A (2001) Multiple walking speed-frequency relations are predicted by constrained optimization. J Theor Biol 209(4):445–453

Bianchi L, Angelini D, Orani GP, Lacquaniti F (1998) Kinematic coordination in human gait: relation to mechanical energy cost. J Neurophysiol 79(4):2155–2170

Borghese NA, Bianchi L, Lacquaniti F (1996) Kinematic determinants of human locomotion. J Physiol 494(3):863–879

Bruijn SM, van Dieën JH, Meijer OG, Beek PJ (2009) Statistical precision and sensitivity of measures of dynamic gait stability. J Neurosci Methods 178(2):327–333

Bruijn SM, Bregman DJ, Meijer OG, Beek PJ, van Dieën JH (2011) The validity of stability measures: a modelling approach. J Biomech 44(13):2401–2408

Bruijn SM, Bregman DJ, Meijer OG, Beek PJ, van Dieën JH (2012) Maximum Lyapunov exponents as predictors of global gait stability: a modelling approach. Med Eng Phys 34(4):428–436

Clark DJ, Ting LH, Zajac FE, Neptune RR, Kautz SA (2010) Merging of healthy motor modules predicts reduced locomotor performance and muscle coordination complexity post-stroke. J Neurophysiol 103(2):844–857

Courtine G, Schieppati M (2004) Tuning of a basic coordination pattern constructs straight-ahead and curved walking in humans. J Neurophysiol 91(4):1524–1535

d'Avella A, Saltiel P, Bizzi E (2003) Combinations of muscle synergies in the construction of a natural motor behavior. Nat Neurosci 6(3):300–308

Dingwell JB, Cusumano JP (2000) Nonlinear time series analysis of normal and pathological human walking. Chaos 10(4):848–863

Dingwell JB, Kang HG (2007) Differences between local and orbital dynamic stability during human walking. J Biomech Eng 129(4):586–593

Dingwell JB, Marin LC (2006) Kinematic variability and local dynamic stability of upper body motions when walking at different speeds. J Biomech 39(3):444–452

Dingwell JB, Cusumano JP, Sternad D, Cavanagh PR (2000) Slower speeds in patients with diabetic neuropathy lead to improved local dynamic stability of continuous overground walking. J Biomech 33(10):1269–1277

Doke J, Donelan JM, Kuo AD (2005) Mechanics and energetics of swinging the human leg. J Exp Biol 208(3):439–445

Donelan JM, Kram R, Kuo AD (2001) Mechanical and metabolic determinants of the preferred step width in human walking. Proc Biol Sci 268(1480):1985–1992

Elble RJ, Thomas SS, Higgins C, Colliver J (1991) Stride-dependent changes in gait of older people. J Neurol 238(1):1–5

England SA, Granata KP (2007) The influence of gait speed on local dynamic stability of walking. Gait Posture 25(2):172–178

Fraser AM, Swinney HL (1986) Independent coordinates for strange attractors from mutual information. Phys Rev A Gen Phys 33(2):1134–1140

Funato T, Aoi S, Oshima H, Tsuchiya K (2010) Variant and invariant patterns embedded in human locomotion through whole body kinematic coordination. Exp Brain Res 205(4):497–511

Funato T, Aoi S, Tomita N, Tsuchiya K (2015) Validating the feedback control of intersegmental coordination by fluctuation analysis of disturbed walking. Exp Brain Res 233(5):1421–1432

Gottschall JS, Kram R (2005) Energy cost and muscular activity required for leg swing during walking. J Appl Physiol (1985) 99(1):23–30

Grasso R, Bianchi L, Lacquaniti F (1998) Motor patterns for human gait: backward versus forward locomotion. J Neurophysiol 80(4):868–885

Hagio S, Kouzaki M (2014) The flexible recruitment of muscle synergies depends on the required force-generating capability. J Neurophysiol 112(2):316–327

Hagio S, Fukuda M, Kouzaki M (2015) Identification of muscle synergies associated with gait transition in humans. Front Hum Neurosci 9:48

Hak L, Houdijk H, Beek PJ, van Dieën JH (2013) Steps to take to enhance gait stability: the effect of stride frequency, stride length, and walking speed on local dynamic stability and margins of stability. PLoS One 8:12

Hoogkamer W, Bruijn SM, Sunaert S, Swinnen SP, Van Calenbergh F, Duysens J (2015) Toward new sensitive measures to evaluate gait stability in focal cerebellar lesion patients. Gait Posture 41(2):592–596

Huang Y, Vanderborght B, Van Ham R, Wang Q (2014) Torque–stiffness-controlled dynamic walking with central pattern generators. Biol Cybern 108(6):803–823

Huang Y, Huang Q, Wang Q (2017) Chaos and bifurcation control of torque- stiffness-controlled dynamic bipedal walking. IEEE Trans Syst Man Cybern Syst 47(7):1229–1240

Ivanenko YP, Grasso R, Macellari V, Lacquaniti F (2002) Control of foot trajectory in human locomotion: role of ground contact forces in simulated reduced gravity. J Neurophysiol 87(6):3070–3089

Ivanenko YP, Cappellini G, Dominici N, Poppele RE, Lacquaniti F (2007) Modular control of limb movements during human locomotion. J Neurosci 27(41):11149–11161

Judge JO, Davis RB, Ounpuu SJ (1996) Step length reductions in advanced age: the role of ankle and hip kinetics. J Gerontol A Biol Sci Med Sci 51(6):303–312

Kang HG, Dingwell JB (2008) Effects of walking speed, strength and range of motion on gait stability in healthy older adults. J Biomech 41(14):2899–2905

Kennel MB, Brown R, Abarbanel HD (1992) Determining embedding dimension for phase-space reconstruction using a geometrical construction. Phys Rev A 45(6):3403–3411

Kerrigan DC, Todd MK, Della Croce U, Lipsitz LA, Collins JJ (1998) Biomechanical gait alterations independent of speed in the healthy elderly: evidence for specific limiting impairments. Arch Phys Med Rehabil 79(3):317–322

Kibushi B, Hagio S, Moritani T, Kouzaki M (2018) Speed-dependent modulation of muscle activity based on muscle synergies during treadmill walking. Front Hum Neurosci 12:4

Kubo A, Hagio S, Kibushi B, Moritani T, Kouzaki M (2017) action direction of muscle synergies in voluntary multi-directional postural control. Front Hum Neurosci 11:434

Kuo AD (2001) A simple model of bipedal walking predicts the preferred speed-step length relationship. J Biomech Eng 123(3):264–269

Kurz MJ, Markopoulou K, Stergiou N (2010) Attractor divergence as a metric for assessing walking balance. Nonlinear Dyn Psychol Life Sci 14(2):151–164

Labini FS, Meli A, Ivanenko YP, Tufarelli D (2012) Recurrence quantification analysis of gait in normal and hypovestibular subjects. Gait Posture 35(1):48–55

Lacquaniti F, Grasso R, Zago M (1999) Motor Patterns in Walking. News Physiol Sci 14:168–174

Lim Y, Lin YC, Pandy MG (2017) Effects of step length and step frequency on lower-limb muscle function in human gait. J Biomech 57:1–7

Liu MQ, Anderson FC, Schwartz MH, Delp SL (2008) Muscle contributions to support and progression over a range of walking speeds. J Biomech 41(15):3243–3252

Lockhart TE, Liu J (2008) Differentiating fall-prone and healthy adults using local dynamic stability. Ergonomics 51(12):1860–1872

Martin PE, Marsh AP (1992) Step length and frequency effects on ground reaction forces during walking. J Biomech 25(10):1237–1239

McAndrew Young PM, Dingwell JB (2012) Voluntary changes in step width and step length during human walking affect dynamic margins of stability. Gait Posture 36(2):219–224

McGowan CP, Neptune RR, Clark DJ, Kautz SA (2010) Modular control of human walking: adaptations to altered mechanical demands. J Biomech 43(3):412–419

Neptune RR, Clark DJ, Kautz SA (2009) Modular control of human walking: a simulation study. J Biomech 42(9):1282–1287

Nishida K, Hagio S, Kibushi B, Moritani T, Kouzaki M (2017) Comparison of muscle synergies for running between different foot strike patterns. PLoS One 12:e0171535

Pires NJ, Lay BS, Rubenson J (2014) Joint-level mechanics of the walk-to-run transition in humans. J Exp Biol 217(19):3519–3527

Prilutsky BI, Gregor RJ (2001) Swing-and support-related muscle actions differentially trigger human walk–run and run–walk transitions. J Exp Biol 204(13):2277–2287

Rosenstein MT, Collins JJ, De Luca CJ (1993) A practical method for calculating largest Lyapunov exponents from small data sets. Phys D 65:117–134

Sano H, Wada T (2017) Knee motion generation method for transfemoral prosthesis based on kinematic synergy and inertial motion. IEEE Trans Neural Syst Rehabil Eng 25(12):2387–2397

Santuz A, Ekizos A, Eckardt N, Kibele A, Arampatzis A (2018) Challenging human locomotion: stability and modular organisation in unsteady conditions. Sci Rep 8(1):2740

Snaterse M, Ton R, Kuo AD, Donelan JM (2011) Distinct fast and slow processes contribute to the selection of preferred step frequency during human walking. J Appl Physiol 110(6):1682–1690

Steele KM, Rozumalski A, Schwartz MH (2015) Muscle synergies and complexity of neuromuscular control during gait in cerebral palsy. Dev Med Child Neurol 57(12):1176–1782

Tresch MC, Saltiel P, Bizzi E (1999) The construction of movement by the spinal cord. Nat Neurosci 2(2):162–167

van Schooten KS, Rispens SM, Pijnappels M, Daffertshofer A, van Dieen JH (2013) Assessing gait stability: the influence of state space reconstruction on inter-and intra-day reliability of local dynamic stability during over-ground walking. J Biomech 46(1):137–141

Vaughan CL, Langerak NG, O'Malley MJ (2003) Neuromaturation of human locomotion revealed by non-dimensional scaling. Exp Brain Res 153(1):123–127

Wu AR, Kuo AD (2016) Determinants of preferred ground clearance during swing phase of human walking. J Exp Biol 219(19):3106–3113